The exceptional sensitivity of brain mitochondria to copper

Sabine Borchard[a], Francesca Bork[a], Tamara Rieder[b], Carola Eberhagen[a], Bastian Popper[c], Josef Lichtmannegger[a], Sabine Schmitt[b], Jerzy Adamski[d], Martin Klingenspor[e,f], Karl-Heinz Weiss[g], Hans Zischka[a,b,*]

[a] Institute of Molecular Toxicology and Pharmacology, Helmholtz Center Munich, German Research Center for Environmental Health, Ingolstaedter Landstrasse 1, D-85764 Neuherberg, Germany
[b] Institute of Toxicology and Environmental Hygiene, Technical University Munich, Biedersteiner Strasse 29, D-80802 Munich, Germany
[c] Department of Anatomy and Cell Biology, Biomedical Center, Ludwig-Maximilians-University Munich, Grosshaderner Strasse 9, D-82152 Planegg-Martinsried, Germany
[d] Institute of Experimental Genetics, Genome Analysis Center, Helmholtz Center Munich, German Research Center for Environmental Health, Ingolstaedter Landstrasse 1, D-85764 Neuherberg, Germany
[e] Chair of Molecular Nutritional Medicine, Technical University of Munich, TUM School of Life Sciences, Weihenstephan, Gregor-Mendel-Strasse 2, D-85354 Freising, Germany
[f] EKFZ - Else-Kröner Fresenius Center for Nutritional Medicine, Technical University of Munich, Gregor-Mendel-Strasse 2, D-85354 Freising, Germany
[g] Department of Gastroenterology, Internal Medicine IV, University Hospital Heidelberg, Im Neuenheimer Feld 110, D-69120 Heidelberg, Germany

ARTICLE INFO

ABSTRACT

Wilson disease (WD) is characterized by a disrupted copper homeostasis resulting in dramatically increased copper levels, mainly in liver and brain. While copper damage to mitochondria is an established feature in WD livers, much less is known about such detrimental copper effects in other organs. We therefore assessed the mitochondrial sensitivity to copper in a tissue specific manner, namely of isolated rat liver, kidney, heart, and brain mitochondria. Brain mitochondria presented with exceptional copper sensitivity, as evidenced by a comparatively early membrane potential loss, profound structural changes already at low copper dose, and a dose-dependent reduced capacity to produce ATP. This sensitivity was likely due to a copper-dependent attack on free protein thiols and due to a decreased copper reactive defense system, as further evidenced in neuroblastoma SHSY5Y cells. In contrast, an increased production of reactive oxygen species was found to be a late-stage event, only occurring in destroyed mitochondria. We therefore propose mitochondrial protein thiols as major targets of mitochondrial copper toxicity.

1. Introduction

The transition metal copper is essential for higher eukaryote's life in its function as cofactor of vital enzymes like the mitochondrial cytochrome *c* oxidase. Despite their copper need, however, cellular copper overload is highly detrimental to mitochondria. This is best exemplified in Wilson disease (WD), a rare genetic disorder characterized by mutations in the *ATP7B* gene encoding a copper excreting ATPase (Bull et al., 1993; Sternlieb and Feldmann, 1976; Tanzi et al., 1993). ATP7B is primarily expressed in the liver and *ATP7B* mutations cause a progressive hepatic copper burden that prominently attacks liver mitochondria (Zischka and Lichtmannegger, 2014). Early on, copper increasingly affects the mitochondrial structure, attacks mitochondrial proteins that are essentially involved in bioenergetic functions, leads to a concomitant decrease in their ATP production capacity, and upon overload culminates in mitochondrial destruction in hepatocytes (Lichtmannegger et al., 2016; Zischka et al., 2011). Such copper-induced mitochondrial dysfunction and destruction provokes hepatic failure that causes death, as demonstrated in *Atp7b*$^{-/-}$ rats, a stringent animal model for severe hepatic WD (Lichtmannegger et al., 2016; Zischka et al., 2011).

In comparison to this massive liver affection, heart abnormalities are rare and renal damage may only be a late, end-stage clinical event in WD (Ala et al., 2007; Bearn et al., 1957; Walshe, 2007). However, the
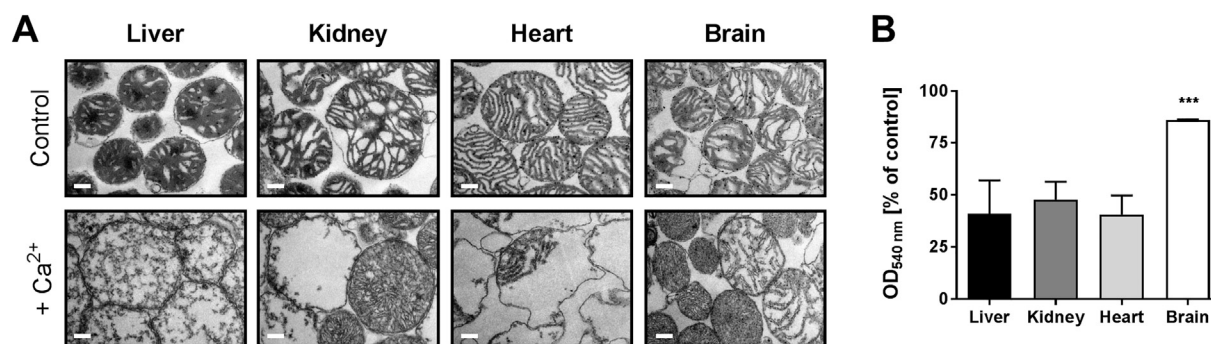
Fig. 1. Isolated mitochondria from rat liver, kidney, heart and brain reveal organ-specific features in response to calcium. (A) Electron micrographs of mitochondria isolated in parallel from rat liver, kidney, heart and brain tissues show comparable high purities and intact inner and outer membranes but organ-specific structural features. A 100 µM Ca^{2+} challenge for 90 min results in mitoplast formation in liver, kidney and heart mitochondria, i.e., enlarged inner membrane vesicles with highly electron-transmissive matrices and disrupted or depleted outer membranes. Such mitoplast formations are mostly absent in equally treated brain mitochondria. Scale bars equal 500 nm. (B) Extent of swelling under calcium challenge is similar between liver, kidney and heart mitochondria, but significantly reduced in brain mitochondria ($N = 3$, $n = 3$). ***$p < .001$ compared to liver, kidney and heart.

brain is severely affected in WD as well (Litwin et al., 2013; Lorincz, 2010). But, in contrast to the liver phenotype of WD, copper toxicity in the brain is much less understood. This is largely due to the lack of suitable animal models that mirror the brain phenotype in WD patients. Massive elevations in brain copper have been reported in WD patients (Litwin et al., 2013), especially in the lentiform nucleus, a collective name for putamen and globus pallidus (Cumings, 1948). The heavy metal accumulation in the brain is associated with neurological impairments, as WD patients present with tremor, Parkinsonism, gait disturbances, dysarthria or seizures (Ala et al., 2007). The current consensus holds that the deleterious brain effects in WD are secondary to liver affection. Originating from excessive liver copper load and/or from dying hepatocytes, a copper spill-over into the bloodstream may impact on the brain (Pfeiffer, 2007; Roberts and Schilsky, 2008). Indeed, several reports have demonstrated improvements of neurological symptoms upon liver transplantation (Catana and Medici, 2012; Schumacher et al., 2001; Weiss et al., 2013), suggesting that restoration of a physiological copper excretion via the liver transplant may also reduce excess brain copper.

From these findings one can hypothesize that mitochondria in other tissues than liver may also be key targets for excessive copper amounts, especially in brain. Kidney, heart or brain may vary from liver in their copper uptake, storage, distribution, and excretion pathways. Nevertheless, different sensitivities or damage extents of their respective mitochondria in response to an increasing copper burden may add to a tissue specific affection in WD. This is plausible, because the molecular composition of mitochondria, e.g., their respective proteomes, is tissue specific (Fernández-Vizarra et al., 2011; Mootha et al., 2003; Wang et al., 2011). As copper primarily attacks sensitive mitochondrial proteins (Banci et al., 2011; Hosseini et al., 2014; Zischka et al., 2011), a tissue specific mitochondrial vulnerability may consequently arise.

We therefore evaluated the sensitivity of mitochondria isolated in parallel from these tissues to comparatively increasing copper challenges and report here that brain mitochondria are especially vulnerable to copper.

2. Materials and methods

2.1. Animals

Heterozygous LPP rats were provided by Jimo Borjigin (University of Michigan, USA). Animals were housed under the guidelines for the care and use of laboratory animals at the Helmholtz Center Munich.

2.2. Cell culture

The human neuroblastoma SHSY5Y and glioblastoma U87MG cell lines were from ATCC (Wesel, Germany) and were cultured in minimum essential medium (MEM) with 1.9 mM GlutaMAX™ containing 5.5 mM glucose supplemented with 10% FCS (Biochrom, Germany), 1% non-essential amino acids, 1% sodium pyruvate and 1% antibiotic-anti-mycotic (Life Technologies, Germany). The cells were maintained at 37 °C in a humidified atmosphere with 5% CO_2. For copper challenge experiments, cells were incubated for 48 h with 0.25 µmol (corresponds to 500 µM) or 0.67 µmol (corresponds to 1340 µM) copper histidine (CuHis)/1×10^5 cells, respectively, comparable to copper concentrations found in brains of Wilson disease patients (ranging from 297 µM to 1092 µM) (Lai and Blass, 1984). Differentiation of SHSY5Y and U87MG was performed as previously described (Das et al., 2008; Encinas et al., 2000) and copper challenge experiments were done as above.

2.3. Mitochondrial preparation

Mitochondria from heterozygous LPP rat liver, kidney, heart and brain were isolated as recently reported (Schulz et al., 2015). Briefly, rat organs were rinsed with ice-cold 0.9% NaCl, placed in ice-cold isolation buffer containing BSA (0.3 M sucrose, 5 mM TES, 0.2 mM EGTA, 0.1% BSA (w/v), pH 7.2), and cleared from surrounding tissue and blood. Liver, kidney and brain were homogenized using a Teflon-glass homogenizer with 5–10 strokes at 800 rpm. Rat heart was minced and manually homogenized in a rough glass-in-glass homogenizer with 5 strokes. All tissue homogenates were centrifuged twice at 800 ×g for clearance of cell debris and nuclei. From the supernatant liver, kidney and heart mitochondria were pelleted at 9000 ×g, but brain mitochondria at 20000 ×g, as they are mostly contaminated with low density myelin. The resulting crude mitochondrial fractions were further purified by density gradient centrifugation at 9000 ×g using an 18/30/60% Percoll™ gradient system for rat liver and kidney mitochondria. Brain and heart mitochondria were resuspended in the 18% Percoll™ solution and placed over a 30/60% gradient and centrifuged at 29000 ×g. The purified organelles were washed and resuspended in isolation buffer without BSA. These tissue specific isolations did result in highly comparable mitochondrial populations with respect to purity (Fig. 1A control, Fig. 3 GSH) and integrity (Fig. 2A control).

Mitochondria from U87MG and SHSY5Y cells were isolated by a pump-controlled cell rupture system (PCC) as described (Schmitt et al., 2013). Briefly, cell suspensions were pumped 3 times through the PCC (clearance: 6 µm, flow rate: 1400 µl/min) and the homogenate was centrifuged at 800 ×g (10 min, 4 °C) for clearing of cell debris and

A

Δψ$_m$ loss max [minutes]

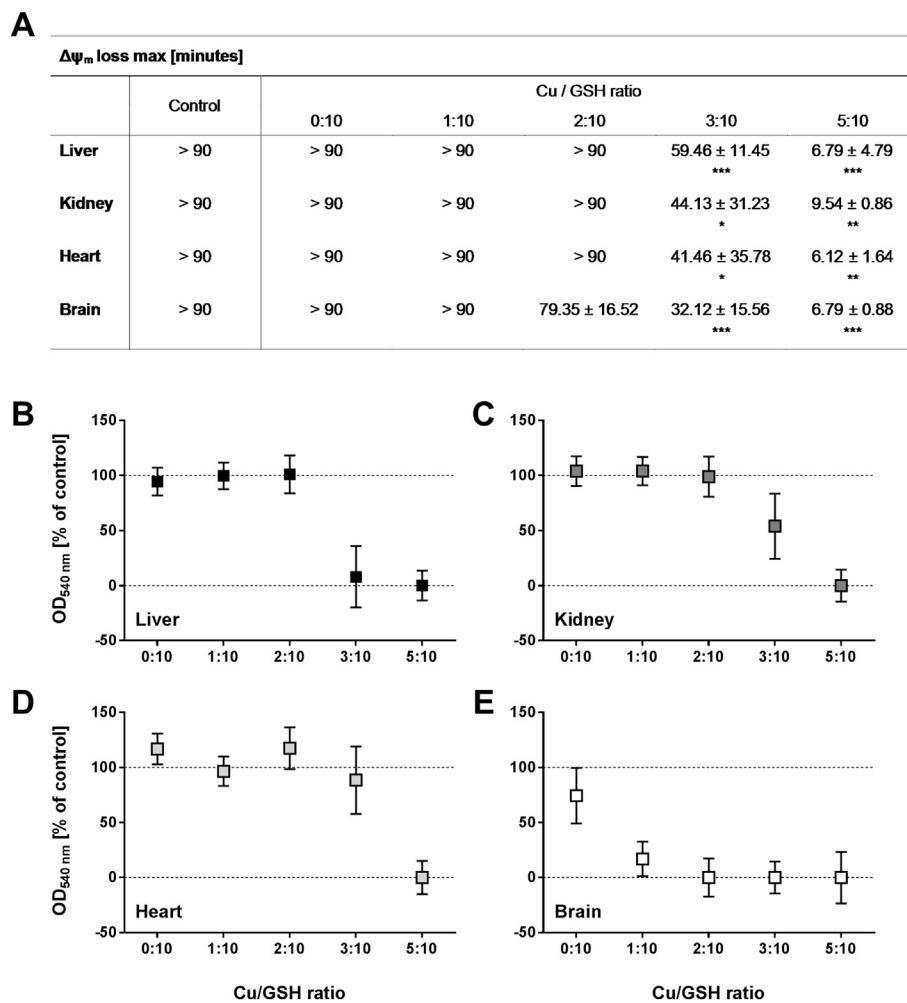|	Control	Cu / GSH ratio				
		0:10	1:10	2:10	3:10	5:10
Liver	> 90	> 90	> 90	> 90	59.46 ± 11.45 ***	6.79 ± 4.79 ***
Kidney	> 90	> 90	> 90	> 90	44.13 ± 31.23 *	9.54 ± 0.86 **
Heart	> 90	> 90	> 90	> 90	41.46 ± 35.78 *	6.12 ± 1.64 **
Brain	> 90	> 90	> 90	79.35 ± 16.52	32.12 ± 15.56 ***	6.79 ± 0.88 ***

Fig. 2. Brain mitochondria are highly sensitive to copper challenges. (A) Isolated rat liver, kidney and heart mitochondria lose their membrane potential (Δψ$_m$) at copper/GSH ratios of 3:10 and 5:10 but exhibit a stable Δψ$_m$ at lower metal concentrations for at least 90 min. In contrast, brain mitochondria lose their membrane potential at lower copper/GSH ratios (2:10) (N = 3, n = 3). *p < .05; **p < .01; ***p < .001 compared to control conditions. (B - D) At copper/GSH ratios up to 2:10, liver, kidney and heart mitochondria show no OD$_{540 nm}$ loss within 90 min. In contrast, brain mitochondria reveal a higher sensitivity to copper as shown by OD$_{540 nm}$ loss at copper/GSH ratio of 1:10 (N = 3, n = 3). For the sake of comparability, 100% OD values are the respective maxima of the mitochondrial suspension, whereas 0% values were set as the lowest OD$_{540 nm}$ values derived from 100 μM Ca^{2+} treatments (Fig. 1B).

nuclei. Subsequently, mitochondria were pelleted at 9000 ×g.

2.4. Functional analysis of isolated mitochondria

Intracellular copper is typically in the monovalent state ("cuprous" Cu^{1+}), in contrast to an extracellular bivalent state ("cupric" Cu^{2+}) (Kim et al., 2008; Knöpfel and Solioz, 2002). In order to mimic intracellular copper exposure, we challenged mitochondria isolated from respective organs or from cell culture with pre-mixed solutions of Cu^{2+} and glutathione (GSH), the major intracellular reductant. Cu^{2+} causes stoichiometric oxidation of GSH to GSSG (Ciriolo et al., 1990). The resulting Cu^{1+} forms complexes with the remaining GSH to give Cu^{1+}-[GSH]$_2$ complexes (2 Cu^{2+} + 6 GSH → 2 Cu^{1+}-[GSH]$_2$ + GSSG) (Brose et al., 2014; Speisky et al., 2009). Thus, at ratios of copper/GSH below 3:10 (corresponding to 300 μM copper and 1 mM GSH), cuprous copper (Cu^{1+}) largely predominates in these complexes, with cupric Cu^{2+} well below 1% as determined by EPR spectroscopy (Ciriolo et al., 1990). As GSH is also a physiological copper binding molecule (Banci et al., 2010) this setting therefore mimics intracellularly increased but GSH bound Cu^{1+} levels. At strongly elevated copper, e.g., at a copper/GSH ratio of 5:10, GSH becomes limiting, causing incomplete Cu^{2+} reduction and incomplete GSH complexation. Such a setting therefore mimics conditions of severe copper overload.

The mitochondrial permeability transition (MPT, "swelling") was monitored in mitochondrial suspensions at OD$_{540 nm}$ (Synergy 2, BioTek, USA) in the presence of 5 mM succinate/2 μM rotenone for 90 min (Bernardi et al., 1992; Zischka et al., 2008). OD$_{540 nm}$ values after 90 min of either untreated or Ca^{2+}-treated (100 μM, positive control) mitochondria from the respective tissue were set to 100% or 0%, respectively. Copper-dependent toxicity was analyzed in the presence of 1 mM GSH (Valko et al., 2006) and increasing copper/GSH ratios of 0:10 to 5:10.

Mitochondrial membrane potential (MMP) was monitored by Rhodamine 123 (Rh123) fluorescence (Schulz et al., 2013; Zamzami et al., 2000) for 100 min in the presence of succinate/rotenone. Addition of the protonophore carbonylcyanide-p-(trifluoromethoxy) phenylhydrazone (FCCP, 1 μM) after 90 min served as internal control (Kessler et al., 1976). Quantitative analyses of MMP loss were done as recently described (Schulz et al., 2013).

Hydrogen peroxide production of isolated mitochondria was determined by horseradish peroxidase-catalysed oxidation of Amplex red to fluorescent resorufin as previously described (Einer et al., 2017; Zhou et al., 1997).

Aconitase activity was measured as previously described (Schulz et al., 2006). Briefly, freeze/thawed mitochondrial suspensions were assayed in the presence of the reaction buffer (50 mM Tris-HCl, 60 mM sodium citrate, 1 mM MnCl$_2$, 0.2 mM NADP$^+$, 4 units of NADP$^+$ isocitrate dehydrogenase, pH 7.5) and NADPH formation was monitored at 340 nm for 60 min at 37 °C.

ATP production was measured by the ATP Bioluminescence Assay Kit (Roche, Germany) according to the manufacturer instructions. Mitochondrial suspensions were pre-incubated for 10 min with increasing copper/GSH ratios before the addition of ADP.

2.5. Mitochondrial glutathione and thiol status

GSH/GSSG levels were determined according to (Rahman et al., 2006) with slight modifications. Mitochondrial suspensions from rat liver and brain were mixed with equal volumes of 10% metaphosphoric acid to precipitate proteins and subsequently neutralized by triethanolamine. Total GSH content was assayed without further processing. For GSSG determination, samples were further processed by masking GSH with 9% 2-vinylpyridine. Samples were assayed in the presence of the reaction buffer (0.1 M potassium phosphate, 0.3 mM NADPH, 20 units of glutathione reductase, pH 7.4) and 0.2 mM 5,5′-dithiobis-(2-nitrobenzoic acid) (DTNB). The formation of TNB was quantified at 412 nm.

Mitochondrial thiol levels were measured as previously described (Ellman and Lysko, 1979). Briefly, mitochondrial suspensions were incubated in the presence or absence of 2.5 mM DTT (10 min, RT) or at copper/GSH ratios of 1:5 (100 μM copper/500 μM GSH), 2:10 (200 μM copper/1 mM GSH) or 4:20 (400 μM copper/2 mM GSH) for 30 min at RT, i.e. with increasing absolute Cu^{1+} amounts but at equal "redox ratio" to GSH. Samples were washed twice and accessible free thiols were subsequently quantified by DTNB at 412 nm.

Oxidation of mitochondrial protein thiols was examined by absence of fluorescent labeling using BODIPY FL (Thermo Fisher Scientific, USA). Freshly isolated mitochondria were treated with increasing copper/GSH ratios for 30 min. Proteins were labeled with 0.3 nmol BODIPY FL/μg mitochondrial protein and separated by SDS-PAGE without thiol-reducing agents (Zischka et al., 2011). Fluorescence was detected using a FUSION FX7 detection system (Vilber Lourmat, Germany).

2.6. Functional analysis of mitochondria at the cellular level

The mitochondrial membrane potential was assessed using $DiOC_6$ (Thermo Fisher Scientific, USA) and mitochondrial ROS production was monitored by MitoSOX™ (Thermo Fisher Scientific, USA). 1×10^5 cells were either stained with 20 nM $DiOC_6$ or 5 μM MitoSOX in PBS for 15 min at 37 °C and fluorescence was detected at 530 nm ($DiOC_6$) or 580 nm (MitoSOX), respectively.

2.7. Electron microscopy

Electron microscopy of isolated mitochondria and cells was done as previously described (Schulz et al., 2013; Zischka et al., 2008) on a 1200EX electron microscope (JEOL, Japan) at 80 kv. Pictures were taken with a KeenView II digital camera (Olympus, Germany) in a blinded way and processed by the iTEM software package (analySIS FIVE, Olympus, Germany). Mitochondrial shape and structure were analyzed identically for all samples using ImageJ. Mitochondria were considered "roundish", when the ratio maximum vs. minimum diameter was < 1.5; otherwise, mitochondria were deemed "elliptical".

2.8. Miscellaneous

Copper in cell suspensions was analyzed by ICP-OES (Ciros Vision, SPECTRO Analytical Instruments, Kleve, Germany) as previously described (Zischka et al., 2011). Protein concentrations were determined by the Bradford assay (Bradford, 1976). Cellular GSH levels were determined as described for mitochondrial GSH determination. For immunoblotting, proteins were transferred to a PDVF membrane and probed with antibodies against 4-hydroxynonenal (1:1000, ab46545, Abcam, UK), citrate synthase (1:1000, 16131-1-AP, Proteintech, USA) and metallothionein (1:1000, ab12228, Abcam, UK). Interference of copper/GSH with fluorescent/luminescent probes was tested negative for all experimental settings.

2.9. Statistics

Throughout this manuscript "N" designates the number of animals (biological replicates) and "n" the number of technical replicates. Data are mean values with standard deviation (SD). Statistical significance was analyzed using 1-way ANOVA with Dunnett's multiple comparisons test (GraphPad Prism 7; GraphPad Software Inc., USA). The differences were considered significant with $*p < 0.05$, $**p < 0.01$, $***p < 0.001$.

3. Results

3.1. Brain mitochondria reveal structural peculiarities and a distinct sensitivity to calcium

In order to directly compare tissue specific sensitivities to potentially damaging insults, mitochondria were isolated from rat liver, kidney, heart, and brain in parallel from the same animals, respectively. Fig. 1A (upper panel) depicts the comparable structural integrity of these isolated mitochondrial populations that typically appeared in the "condensed" state (i.e., with an intact outer membrane, well-defined cristae and electron-dense matrices (Hackenbrock, 1966)). Despite this overall comparability, however, liver mitochondria had a prominent electron-dense matrix, heart mitochondria presented with highly regular and parallel oriented cristae. Kidney mitochondria showed abundant rounded cristae and brain mitochondria had a comparatively slightly reduced size (Fig. 1A).

These tissue specific mitochondrial structural features may be the manifestation of their different molecular compositions (Mootha et al., 2003). Consequently, impacts that directly attack mitochondrial structures may cause differing, potentially tissue specific, mitochondrial damage. As validation for this supposition, we subjected the diverse mitochondrial populations to a 100 μM Ca^{2+} challenge, the prototype inducer of the mitochondrial permeability transition (MPT) (Hunter and Haworth, 1979). As expected, Ca^{2+} caused massive "swelling" and mitoplast formation in liver (Zischka et al., 2008), kidney and heart mitochondria (Fig. 1A, lower panel). Enlarged inner membrane vesicles with electron-transmissive matrices and disrupted or depleted outer membranes resulted with liver mitochondria most homogeneously affected (Fig. 1A, lower panel). In contrast, however, Ca^{2+}-treated brain mitochondria did not present with such typical mitoplast formations (Fig. 1A, lower panel). Heterogeneous mixtures of mitochondria with either electron-transmissive matrices and rather organized cristae, or with uniform greyish numerous small intra-mitochondrial structures were observed (Fig. 1A, lower panel). In accord with these ultrastructural findings, brain mitochondria showed a significantly less pronounced decrease in $OD_{540\ nm}$ upon a Ca^{2+} challenge compared to mitochondria from other tissues (Fig. 1B), in agreement with an earlier report (Berman et al., 2000). Thus, mitochondria may react differently to directly imposed challenges, validating the need to test detrimental impacts on mitochondria in a tissue specific manner.

3.2. Brain mitochondria are highly susceptible to copper

Mitochondria are a prime site for copper utilization, but are also a known key target of detrimental copper overload in liver (Zischka and Lichtmannegger, 2014). In order to assess whether mitochondria from other tissues are equally vulnerable to copper, we compared rat liver, kidney, heart and brain mitochondria freshly isolated in parallel for their copper sensitivity.

As the mitochondrial membrane potential ($\Delta\psi_m$, MMP) is a highly sensitive parameter of organelle damage, we first assessed the effect of an increasing copper/GSH ratio on MMP (Fig. 2A). As described in the method section, at low copper/GSH ratios copper is mainly present as cuprous Cu^{1+}. In contrast, at a high copper/GSH ratio of 5:10 cupric Cu^{2+} prevails. Control incubations of mitochondrial populations in
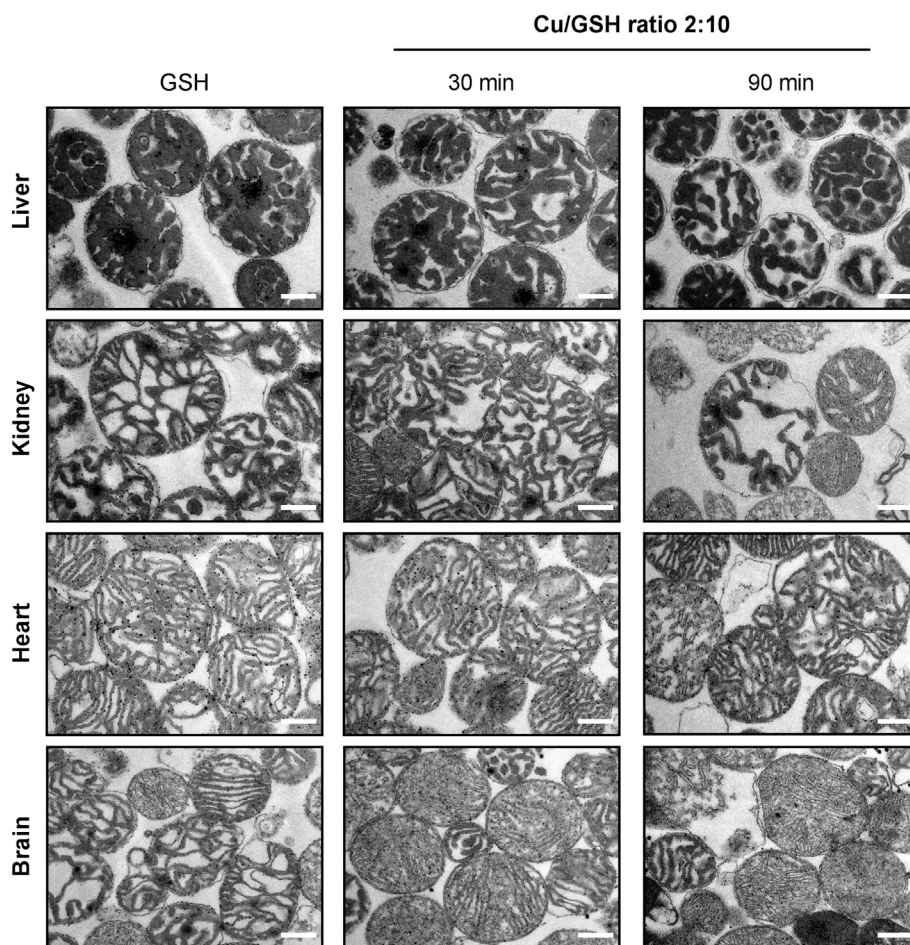
Cu/GSH ratio 2:10

| GSH | 30 min | 90 min |

Fig. 3. Time-dependent mitochondrial structure changes by copper. Cuprous Cu^{1+} induces structural alterations in liver mitochondria reminiscent of observations in liver mitochondria in WD patients and WD animal models. Kidney mitochondria appear with heterogeneous structural alterations but heart mitochondria remain rather unchanged. The most prominent structural alterations appear in brain mitochondria upon copper challenge. Scale bars equal 500 nm.

buffer only, demonstrated a highly stable MMP (> 90 min) in mitochondria from all tissues (Controls, Fig. 2A), validating their functional integrity upon isolation. In contrast, Cu^{2+} (copper/GSH ratio of 5:10) dissipated the MMP in all mitochondrial populations within minutes (Fig. 2A). Thus, Cu^{2+} is highly detrimental to mitochondria in general. Upon exposure to cuprous Cu^{1+} bound to GSH (copper/GSH ratio of 2:10), however, mitochondria from liver, kidney and heart but not from brain exhibited a stable MMP for at least 90 min. Brain mitochondria demonstrated a faster MMP loss, already at 80 min, in contrast to the other mitochondrial populations (Fig. 2A).

Elevated copper sensitivity in brain mitochondrial suspensions was also observed by a strong OD_{540nm} decrease, already at a copper/GSH ratio of 1:10 (Fig. 2E), a comparatively low Cu^{1+} challenge. In fact, liver and kidney mitochondria required at least a threefold higher total copper dose (copper/GSH ratio of 3:10) for a distinct $OD_{540\ nm}$ decrease (Fig. 2B, C). Of note, heart mitochondria appeared highly stable and only showed an $OD_{540\ nm}$ loss at a copper/GSH ratio of 5:10 (Fig. 2D).

This exceptional vulnerability of brain mitochondria to copper could further be visualized by ultra-structural analyses (Fig. 3). Mitochondria were treated with Cu^{1+} (copper/GSH ratio of 2:10) for 30 and 90 min, fixed and subsequently examined by electron microscopy. Liver and kidney mitochondria demonstrated a time-dependent increase in matrix density and cristae dilatation, most prominently upon a 90 min Cu^{1+} challenge (Fig. 3). On the contrary, heart mitochondria were remarkably stable and appeared largely unaltered. In strong contrast, brain mitochondria showed the most distinct structural alterations, already upon a 30 min Cu^{1+} challenge, without worsening

upon a 90 min Cu^{1+} challenge (Fig. 3). Thus, the Cu^{1+}-evoked damage to brain mitochondria occurred and terminated comparatively fast. Cu^{1+}-treated brain mitochondria appeared uniformly greyish with strongly thinned cristae, demonstrating massive structural alterations in comparison to GSH-treated controls (Fig. 3).

3.3. Fenton-chemistry based toxicity is rather a consequence than the cause of mitochondrial impairments by copper

Copper is a redox-active trace element, characterized by its ability to shift between the oxidized Cu^{2+} and the reduced Cu^{1+} state (Kim et al., 2008). While the primary toxin in WD is excess copper, a matter of constant debate is, which of its adverse effects are causative for hepatocyte death. One major hypothesis has been that aqueous free copper could catalyze the formation of highly detrimental reactive oxygen species (ROS) via Fenton- and Haber-Weiss-based chemistry (Stohs and Bagchi, 1995). However, a Fenton-chemistry-based copper toxicity as prime deleterious mechanism in WD has been challenged by thorough calculations demonstrating the lack of free, i.e., unbound copper in cells (Rae et al., 1999). Driven by this discussion, we analyzed, whether an enhanced ROS emergence or damage is present in copper challenged mitochondria that could account for the observed structural and functional impairments (Figs. 2, 3). For the sake of conciseness, we restricted ourselves to the study of the most vulnerable brain and liver mitochondria here.

First, we measured hydrogen peroxide (H_2O_2) emergence from respiring copper-challenged mitochondria (Fig. 4A). Brain mitochondria
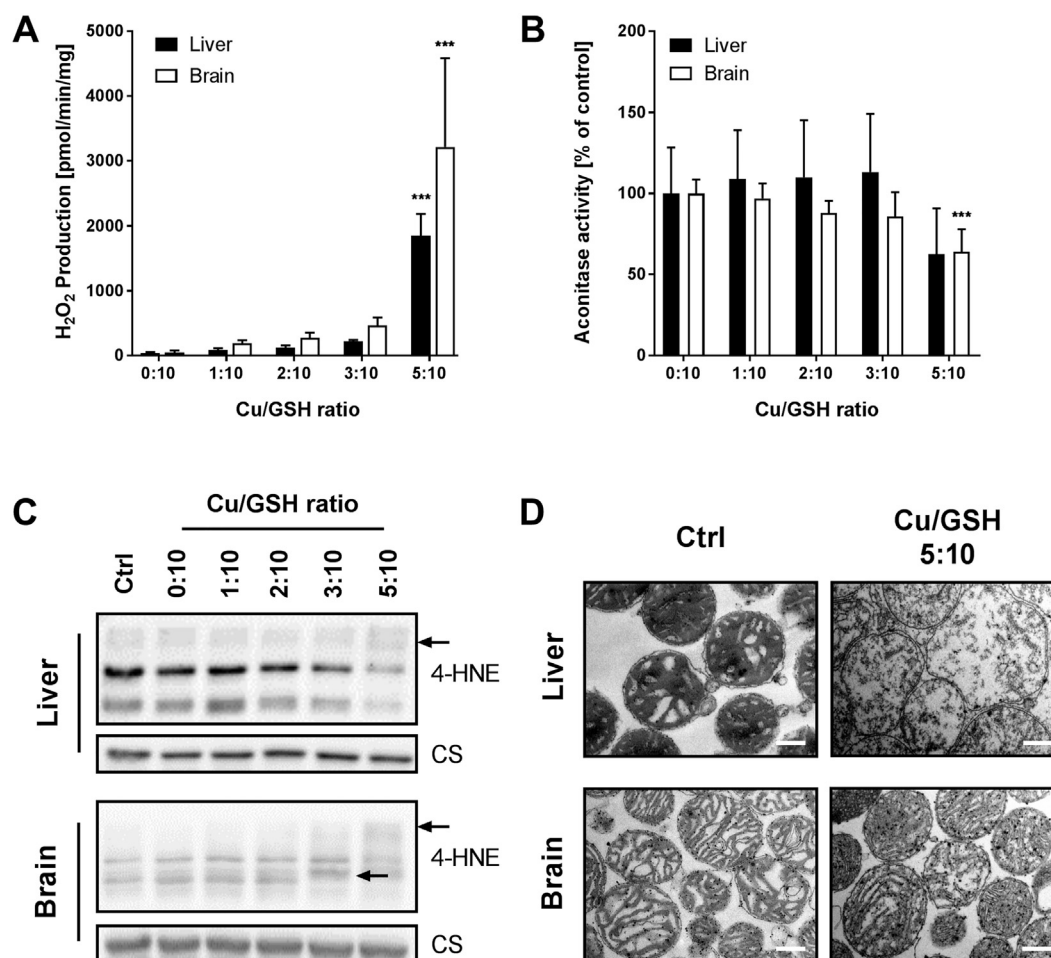
Fig. 4. Massive oxidative stress occurs upon copper induced mitochondrial destruction. (A) The rate of hydrogen peroxide (H_2O_2) production in mitochondria from liver and brain is significantly increased upon challenge with a high copper/GSH ratio of 5:10, a condition that readily destroys mitochondria ($N = 3$, $n = 3$); ***$p < .001$. (B) The mitochondrial aconitase activity is not affected in both, rat liver and brain mitochondria, by copper/GSH ratios up to 3:10 but significantly decreased at the highest copper/GSH ratio ($N = 3–4$, $n = 6–8$); ***$p < .001$. (C) Lipid peroxidation, determined by 4-hydroxynonenal (4-HNE) adduct formation, was increased at the highest copper/GSH ratio but stable at lower ratios in both, liver and brain mitochondria ($N = 3$). (D) The highest copper/GSH ratio (5:10) leads to a massive destruction of liver and brain mitochondria compared to control conditions. Scale bars equal 500 nm.

did produce slightly higher ROS amounts than liver mitochondria at Cu/GSH ratios from 1:10 to 3:10. However, in comparison to the respective controls, these elevations were very low and non-significant for both mitochondrial populations (Fig. 4A). In contrast, a significant and massive ROS emergence in both mitochondrial populations was apparent by incubation with cupric copper (copper/GSH ratio of 5:10). Thus, only excessive copper exposures that readily destroy mitochondria (Fig. 4D) are paralleled by significant mitochondrial ROS emergence.

Second, we analyzed copper-challenged mitochondria for oxidative damage using the redox-sensitive mitochondrial aconitase activity as surrogate (Fig. 4B). No reduced activities in both mitochondrial populations were apparent at Cu/GSH ratios below 5:10, but a significant aconitase activity decrease occurred in the presence of Cu^{2+} (copper/GSH ratio of 5:10, Fig. 4B).

Third, we assessed the formation of 4-hydroxynonenal (4-HNE)-protein adducts as indicator for ROS-initiated lipid peroxidation (Fig. 4C). In brain mitochondria, a slight pattern change of 4-HNE protein adducts appeared at copper/GSH ratio of 3:10, but both mitochondrial populations only showed an unambiguously changed protein pattern at the highest copper/GSH ratio (5:10, Fig. 4C).

Finally, we incubated liver and brain mitochondria with the highest copper/GSH ratio (5:10) and analyzed the structural consequences by electron microscopy (Fig. 4D). Compared to control conditions,

incubation of liver and brain mitochondria with a copper/GSH ratio of 5:10 for 30 min led to a destruction of the organelles. This destruction was characterized by a disruption of the outer mitochondrial membrane and the loss of cristae structure.

Taken together, these results demonstrated that substantial mitochondrial ROS emergence or oxidative damage only occurred at a very high copper/GSH ratio of 5:10, a condition that readily destroyed both mitochondrial populations. Consequently, such pronounced emergence/damage is a late-stage event of mitochondrial copper toxicity in liver and brain mitochondria that does not, however, account for the observed mitochondrial impairments (MMP loss, $OD_{540\ nm}$ decrease, structural damage) at lower copper/GSH ratios.

3.3.1. Mitochondrial protein thiols are primary targets of copper toxicity

We have previously demonstrated that mitochondrial protein thiols are crucial targets of copper toxicity in liver mitochondria (Zischka et al., 2011). Therefore, we determined the amount of accessible free thiols of the most copper-sensitive mitochondria, i.e., from liver and brain (Fig. 5A). Mitochondria were treated with copper/GSH ratios of 1:5, 2:10 or 4:20 for 30 min and accessible free thiols were measured using 5,5′-dithiobis-(2-nitrobenzoic acid) (DTNB). Free thiols of liver and brain mitochondria were depleted by copper/GSH in a dose-dependent manner (Fig. 5A). A significant reduction was present at a ratio of 2:10 (corresponds to 200 μM copper/1 mM GSH), which became
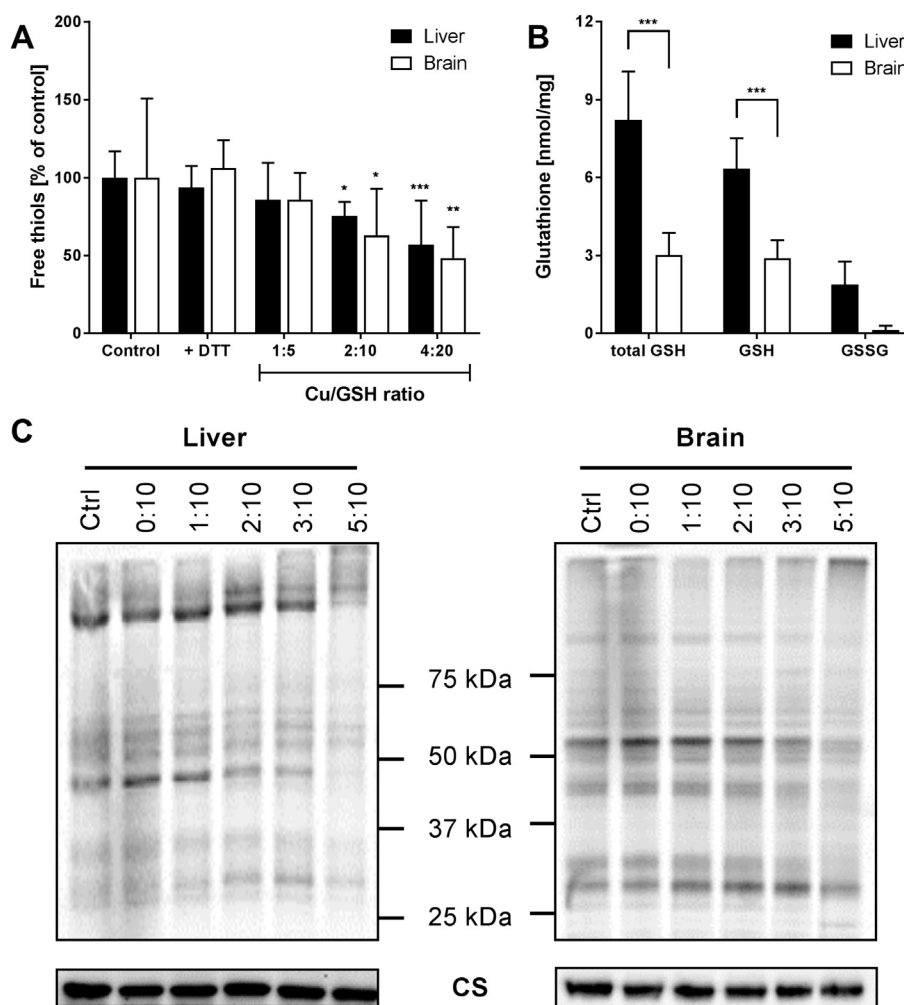
Fig. 5. Free protein thiols are primary targets of copper toxicity in rat liver and brain mitochondria. (A) Free thiols from liver and brain mitochondria are oxidized by copper/GSH in a dose-dependent fashion (N = 5–6); *p < .05, **p < .01, ***p < .001. (B) Rat brain mitochondria reveal a significantly lower total GSH content compared to rat liver mitochondria (N = 5, n = 10). (C) Fluorescent labeling of free protein thiols with BODIPY FL reveals decreased fluorescence intensity of distinct bands with increasing copper/GSH ratios in both, liver and brain mitochondria. Citrate synthase (CS) served as loading control (N = 3).

even more prominent at a ratio of 4:20 (corresponds to 400 μM copper/ 2 mM GSH) in isolated organelles from both organs. This finding was further validated by BODIPY FL labeling of accessible protein thiols (Fig. 5C). Here, mitochondria from liver and brain revealed a dramatically decreased overall fluorescence intensity when treated with the highest copper/GSH ratio (5:10). Lower copper/GSH ratios resulted in a band-specific decrease in fluorescence. Thus, protein thiols are a prominent target in both, liver and brain mitochondria.

Why are brain mitochondria more affected by copper than liver mitochondria? To answer this question, we determined the level of glutathione, the major intracellular protective compound against thiol-oxidative protein damage (Fig. 5B). Here, brain mitochondria revealed a significantly reduced level of total as well as reduced GSH compared to liver mitochondria. Thus, while copper attacks protein thiols in both mitochondrial populations, a significantly lower protective GSH amount may explain a higher susceptibility to copper in brain vs. liver mitochondria.

3.4. Copper impairs the ATP production capacity of brain mitochondria

What are the functional consequences of copper toxicity in liver and brain mitochondria? While liver mitochondrial ATP production capacity is stable at a copper/GSH ratio of 1:10 compared to control conditions, higher ratios resulted in a significant decrease and total loss of

ATP production (Fig. 6A). In contrast, brain mitochondria revealed a striking sensitivity to copper challenges, as their ATP production capacity significantly decreased already at low copper challenges (copper/GSH ratio of 1:10, Fig. 6A).

3.5. SHSY5Y mitochondria are more susceptible than U87MG mitochondria to copper damage

In the above sections we have analyzed mitochondria from total rat brain homogenates. Due to their origin from different cell types in brain, an overall picture was achieved. In more detail, we further analyzed mitochondrial copper sensitivity in two brain derived cell types, the neuroblastoma cell line SHSY5Y and the glioblastoma cell line U87MG as frequently employed surrogates for neurons and glial cells, respectively. Isolated mitochondria from SHSY5Y cells revealed a Cu^{1+} dose-dependent decrease in ATP production capacity when incubated with copper/GSH (ratio 1:10) and a significantly reduced ATP production at the highest copper concentration tested (Fig. 6B). In comparison, organelles from U87MG cells were not affected by such copper challenges (Fig. 6B). To further characterize this different response of SHSY5Y vs. U87MG mitochondria to copper, we treated isolated mitochondria from both cell lines with copper/GSH and labeled free protein thiols with BODIPY FL (Fig. 6C). Treatment of SHSY5Y mitochondria with copper/GSH resulted in a dose-dependent decrease
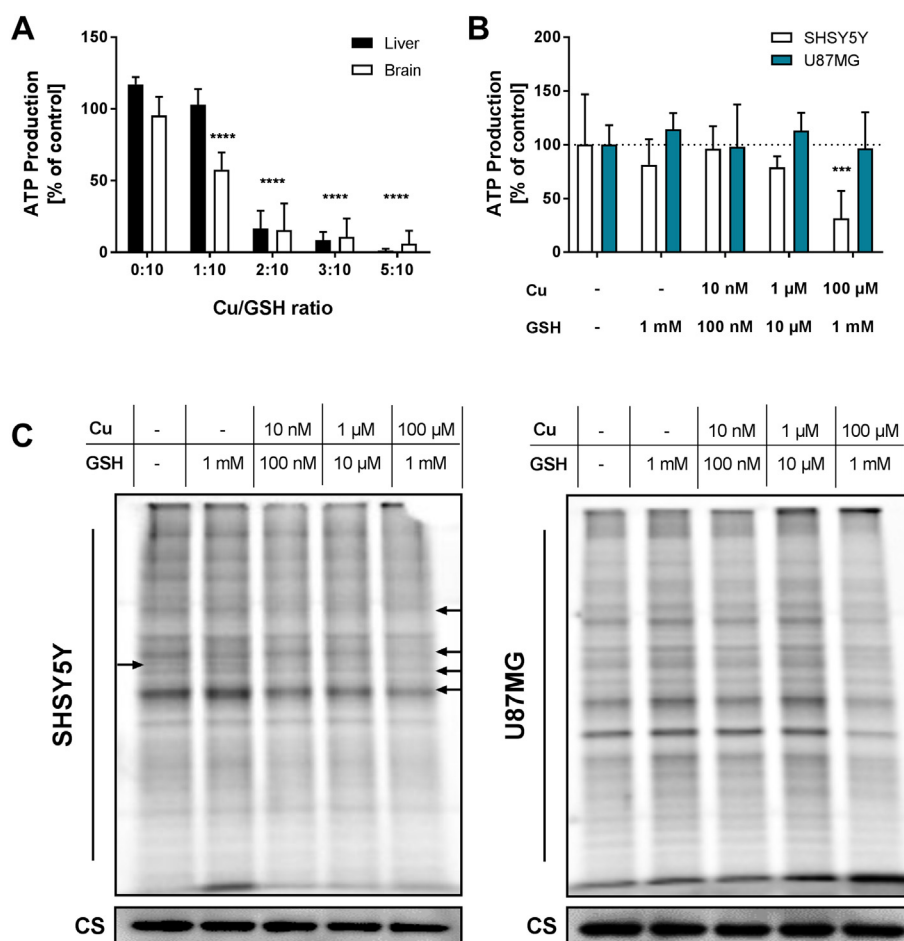
Fig. 6. Copper exposure significantly lowers mitochondrial ATP production capacity. (A) In rat liver mitochondria, ATP production capacity is unchanged at copper/GSH ratio of 1:10, but significantly decreased at copper/GSH ratios ranging from 2:10 up to 5:10 compared to GSH alone. In comparison, brain mitochondria reveal a significantly decreased ATP production capacity even at the lowest copper/GSH ratio of 1:10 (N = 3, n = 6); ***p < .001 compared to the respective control (copper/GSH ratio 0:10). (B) Treatment of isolated mitochondria from SHSY5Y (neuroblastoma) cells with copper/GSH leads to a dose-dependent decrease in ATP production, whereas ATP production of U87MG (glioblastoma) mitochondria is not affected by copper treatment (N = 3–4; n = 6–8); ***p < .001 compared to control conditions. (C) Protein thiols of isolated mitochondria from SHSY5Y and U87MG cells were labeled with BODIPY FL. SHSY5Y mitochondria reveal a dose-dependent decrease of overall fluorescence, whereas U87MG mitochondria show a loss of fluorescence signal only at the highest copper concentration. Citrate synthase (CS) served as loading control (N = 3).

in BODIPY FL-labeled protein fluorescence (Fig. 6C). In contrast, a decrease in fluorescence in U87MG mitochondria was only present at the highest copper concentration (Fig. 6C). Thus, neuroblastomal but not glioblastomal mitochondria are highly sensitive to copper and their free protein thiols are a sensitive target to metal challenges.

3.6. Limited defense mechanisms against copper aggravate mitochondrial impairment in SHSY5Y cells

As isolated mitochondria from SHSY5Y cells were highly sensitive to copper compared to U87MG cells, we aimed to test their copper sensitivity in a cellular context. Both cell lines were treated with 0.25 or 0.67 μmol copper histidine (CuHis)/1 × 10^5 cells for 48 h. Cells were analyzed by electron microscopy for mitochondrial shape alterations and mitochondria were categorized as "roundish" or "elliptical" (Fig. 7A, B). No significant differences were detected in mitochondrial shape in either SHSY5Y or U87MG cells in absence or presence of CuHis. In addition, there were also no changes in mitochondrial number or size for both cell lines (data not shown).

To further analyze the impact of copper on mitochondria from SHSY5Y and U87MG cells, we defined four distinct categories of mitochondrial structure (Fig. 7C). Stage I mitochondria display an intact inner and outer membrane as well as a distinct cristae structure. In contrast, stage II mitochondria are characterized by shortened cristae, whereas stage III mitochondria show even more dissipated cristae as well as membranous deposits. Finally, stage IV mitochondria display a destroyed outer membrane and a complete loss of cristae structure. In the presence of copper histidine, the mitochondrial structure in SHSY5Y cells was massively altered. The amount of stage I mitochondria dose-dependently decreased, whereas the amount of stage II mitochondria

was stable at a CuHis dose of 0.25 μmol/1 × 10^5 cells, but significantly decreased at the higher CuHis dose. Accordingly, the number of stage III and IV mitochondria was dose-dependently increased in copper-treated SHSY5Y cells (Fig. 7D, Supplement Fig. 1).

These structural abnormalities resulted in functional consequences, mainly a decreased mitochondrial membrane potential (Supplement Fig. 2). The relevance of these findings was further validated by differentiating SHSY5Y and U87MG cells (Supplement Fig. 2). SHSY5Y and U87MG cells are neuroblastoma and glioblastoma cells and thus are only surrogates for adult neurons and glia cells. They differ for example in their proliferation behavior, protein expression pattern and morphology from primary neurons and glia (Das et al., 2008; Shipley et al., 2016). Upon differentiation with retinoic acid, however, these cells resemble adult neurons and glial cells with respect to morphological features (e.g., extended long, branched processes) and the upregulation of proteins characteristic for adult neurons (e.g., MAP2, GAP-43, NeuN) (Encinas et al., 2000; Shipley et al., 2016) or astrocytes (e.g., GFAP, S100B) (Das et al., 2008; Xing et al., 2017), respectively. Consequently, we validated their differentiation by an increased abundance of MAP2 for SHSY5Y cells and GFAP for U87MG cells (data not shown). In full agreement with our observations in undifferentiated cells, we observed a dose-dependent decrease of the mitochondrial membrane potential upon copper challenge in differentiated SHSY5Y cells, but a slight increase in differentiated U87MG cells, indicative of mitochondrial hyperpolarization (Supplement Fig. 2). Moreover, whereas a slight decline in mitochondria-originating ROS was observed in differentiated and undifferentiated SHSY5Y cells, the converse tendency was found in differentiated and undifferentiated U87MG cells (Supplement Fig. 2). Thus, especially SHSY5Y cells, whether differentiated or undifferentiated are affected by increasing copper amounts at the
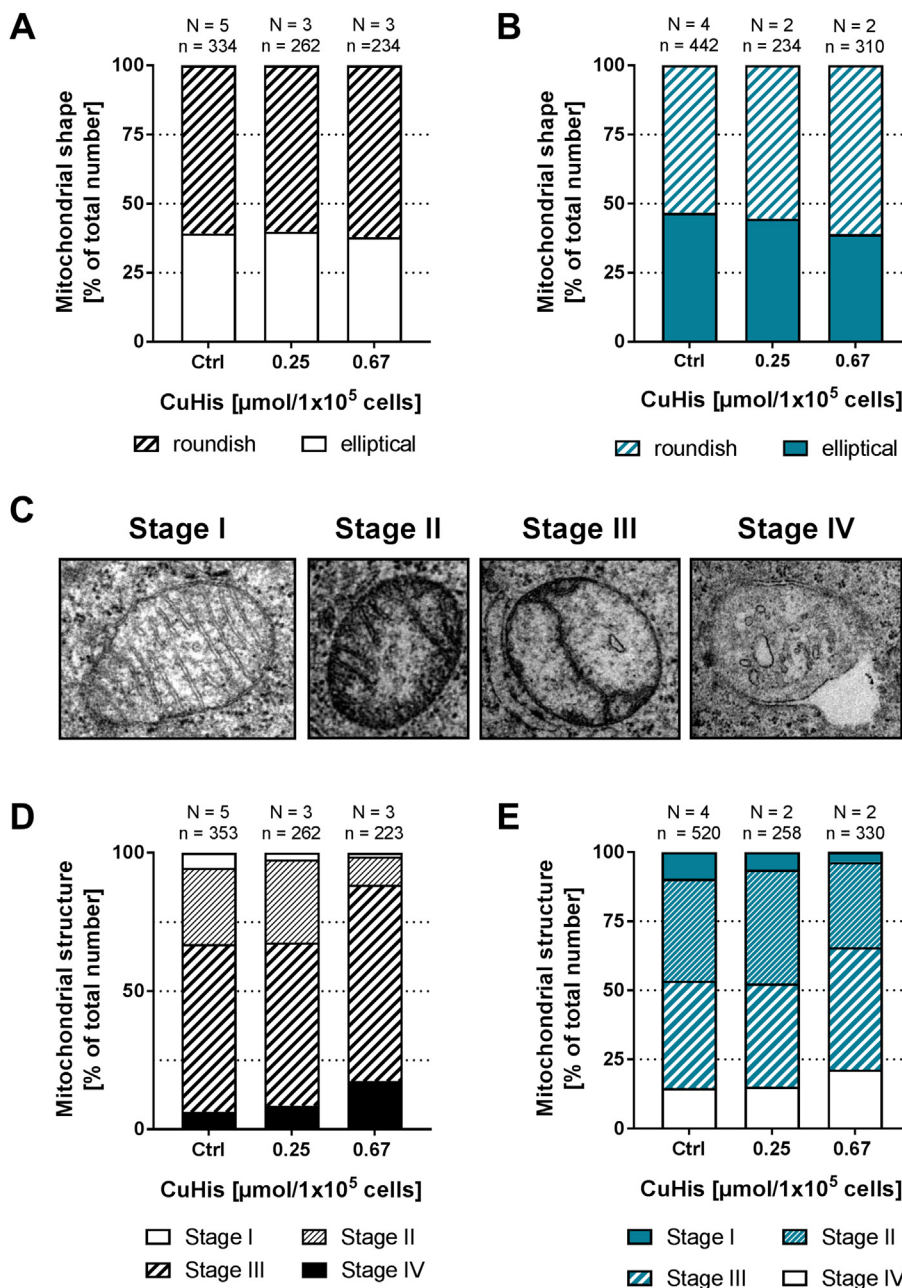
Fig. 7. Mitochondria from SHSY5Y cells are highly susceptible to copper. Mitochondrial shape is not influenced by exposure of copper histidine (CuHis) to SHSY5Y (A) and U87MG (B) cells for 48 h. (C) For further analysis, mitochondria were divided into 4 stages defined by cristae structure, membrane integrity and matrix density. (D) SHSY5Y cells display a dose-dependent increase in stage III and IV mitochondria when incubated for 48 h with CuHis. (E) In U87MG cells, an increase of stage IV mitochondria is only present at the highest CuHis dose.

mitochondrial level.

In contrast to copper-induced mitochondrial structure changes in SHSY5Y cells, mitochondria from U87MG cells (Fig. 7E, Supplement Fig. 1) appeared largely unaffected at the 0.25 μmol CuHis dose and only slightly changed towards decreased stage I and II mitochondria and increased stage III and IV mitochondria at the high copper concentration.

Taking these results together, in contrast to U87MG mitochondria, SHSY5Y mitochondria demonstrated a pronounced copper sensitivity at isolated and in situ level, whether these cells were differentiated or left undifferentiated. We therefore conclude that neuronal mitochondria are exceptionally copper-sensitive.

In order to shed light on the different mitochondrial copper sensitivities in a cellular context, we analyzed metallothionein 1/2 (MT1/2)

and glutathione levels in both cell lines. Metallothionein 1/2, the major endogenous copper-scavenging protein, was not detected in SHSY5Y cells, either undifferentiated (Fig. 8A) or differentiated by retinoic acid (data not shown) even after a copper challenge for 48 h, but was abundantly present in glial U87MG cells (Fig. 8A). Moreover, SHSY5Y revealed a significantly lower amount of GSH compared U87MG cells (Fig. 8A).

To exclude a higher uptake of copper by SHSY5Y cells as potential reason for the higher copper susceptibility of SHSY5Y mitochondria, we measured the copper levels in both cells lines after incubation for 48 h (Fig. 8B). Surprisingly, U87MG cells accumulated significantly more copper (around 10-times) compared to SHSY5Y cells when incubated with 0.67 μmol CuHis/1×10^5 cells. Thus, despite a lower copper accumulation, SHSY5Y cells were highly vulnerable to copper. This is
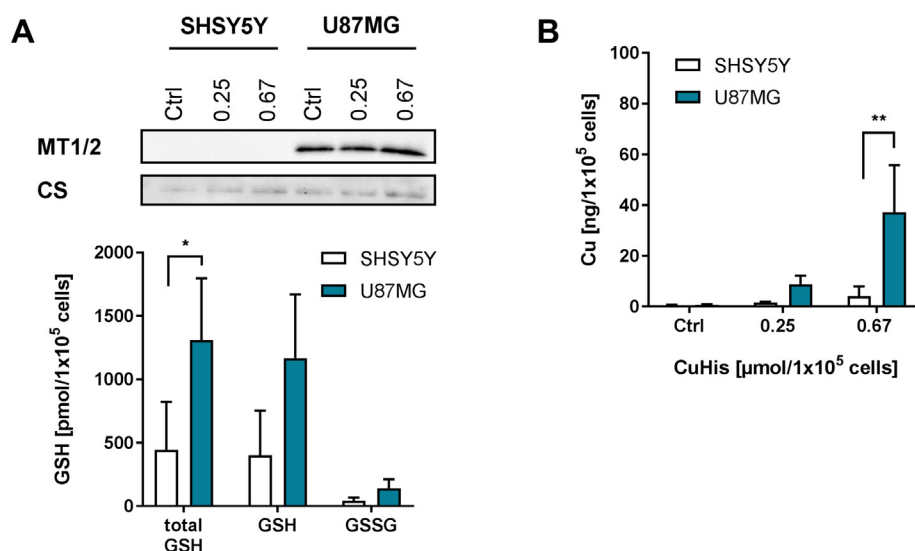
Fig. 8. The high susceptibility of SHSY5Y mitochondrial to copper is attributable to limited defense mechanisms. (A) Immunoblotting against metallothionein 1/2 (MT1/2) shows absence of the copper-binding protein in SHSY5Y cells. In contrast, MT1/2 is present in U87MG cells. Citrate synthase served as loading control. For both cell lines, 1×10^5 cells per lane were applied to a SDS-PAGE (N = 3). Additionally, the total GSH content of untreated SHSY5Y cells is lower compared to U87MG cells (N = 3, n = 3); **p < .01. (B) U87MG cells accumulate significantly more copper in 48 h compared to SHSY5Y cells (N = 3, n = 3).

most plausibly because, in contrast to U87MG cells, SHSY5Y cells have significantly lower levels of the two major cellular anti-copper defense molecules, metallothionein and GSH.

4. Discussion

Wilson disease (WD) is characterized by a disrupted copper homeostasis resulting in dramatically increased copper levels, mainly in liver and brain. Liver mitochondria were identified as pivotal targets of excessive copper burdens in hepatocytes of WD patients (Lichtmannegger et al., 2016; Sternlieb, 1968; Sternlieb, 1978) and WD animal models (Lichtmannegger et al., 2016; Roberts et al., 2008; Zischka et al., 2011). In WD animal livers, a decline in the mitochondrial capacity to produce ATP has been shown to parallel the mitochondrial copper load coinciding with progressive disease states (Lichtmannegger et al., 2016). Most notably, treatments that reduce the mitochondrial copper load avoid hepatocyte death despite still severely augmented copper burdens, e.g., in the cytosol (Lichtmannegger et al., 2016; Zischka et al., 2011). Thus, it is the mitochondrial compartment that decisively contributes to the hepatocyte's faith in WD.

While copper induced mitochondrial impairments can be considered as well established feature in WD livers, much less is known about such detrimental copper effects in other organs. Here, especially the brain is of high interest, as it is severely affected by copper in WD (Członkowska and Schilsky, 2017; Lorincz, 2010). Already in 1961, neurotoxicity of copper in cat brains was demonstrated (Vogel and Evans, 1961). Furthermore, using explanted brain tissues ranging from mice to monkey, neuronal copper intoxications were demonstrated to cause massively increased oxygen consumption. The authors attributed this accelerated respiration to a strong uncoupling of affected neuronal mitochondria and concluded that in the brain, mitochondria are highly vulnerable to copper (Vogel and Kemper, 1963). While these early studies clearly indicated an important role of mitochondrial impairment in copper induced brain damage, unfortunately, further studies along this line are largely missing.

We therefore aimed to test the direct sensitivity of mitochondria from different tissues to copper. While liver, kidney, heart, and brain surely differ in their cellular copper homoeostasis, the present study is a "bottom-up" approach addressing the question, if mitochondria from these tissues would be confronted with equal copper challenges, would they be damaged equally or differently? Indeed, it is reasonable to assume a tissue specific mitochondrial copper sensitivity, as these organelles markedly differ in their structure (Fig. 1A), their molecular composition (Fernández-Vizarra et al., 2011; Mootha et al., 2003; Wang

et al., 2011), and their sensitivities to applied challenges, as exemplified by calcium (Fig. 1B).

We report here an especially high sensitivity of brain mitochondria to cuprous copper (Cu^{1+}). Brain mitochondria presented with a comparatively early MMP loss (Fig. 2A), profound structural changes already at low Cu^{1+} (Figs. 2E, 3), and a Cu^{1+} dose-dependent reduced capacity to produce ATP (Fig. 6A).

Of note, especially in brain mitochondria, OD_{540nm} changes were observed at lower Cu/GSH ratios than a beginning loss of membrane potential (Fig. 2). Typically, OD_{540nm} changes are used to assess large amplitude mitochondrial swelling, e.g. induced by calcium that initiates the mitochondrial permeability transition (Zischka et al., 2008). Such swelling is slightly preceded/paralleled by a membrane potential loss (Schulz et al., 2013). However, the OD_{540nm} of a mitochondrial suspension is a summation parameter, which is directly dependent on their light refractive properties (Nicholls and Ferguson, 1992). Consequently, substantial alterations in mitochondrial structure, other than the mitochondrial permeability transition, are detected as well. Indeed, brain mitochondria, in strong contrast to the other mitochondrial populations, showed the most distinct structural alterations, already upon a 30 min Cu^{1+} challenge (Fig. 3). They appeared uniformly greyish with strongly thinned cristae. It further appears that the thinned cristae are nevertheless able to sustain an intact membrane potential, thereby plausibly explaining that a change in OD_{540nm} was assessed already at a Cu/GSH ratio of 1:10 but a membrane potential loss at 2:10, again indicating an exceptional vulnerability of brain mitochondria to copper.

These structural and functional impairments could not be explained by a Fenton-reaction-based chemistry of copper. Indeed, clear cut mitochondrial oxidative damage, assessed by a reduced aconitase activity (Fig. 4B) and lipid peroxidation derived protein adducts (Fig. 4C), was only observed at high dosed copper (Cu^{2+}) challenges. Such conditions, however, readily destroy mitochondria as evidenced by electron microscopy (Fig. 4D), and are also paralleled by a burst of mitochondria derived ROS (Fig. 4A). Thus, liver and brain mitochondria produce significant ROS AFTER their disintegration by excess copper. Several explanations can account for this finding. First, copper-caused disintegration of the highly organized electron transport chain (Korshunov et al., 1997) may lead to electron leakage causing massive ROS (especially at complexes I and III (Murphy, 2009)). Second, copper damage to the respiratory chain complex IV may drastically impair its well-ordered reduction of oxygen to water thereby generating ROS. Third, the high presence of either Cu^{2+} or loosely bound Cu^{1+} may react in a Fenton-chemistry based manner to generate highly detrimental hydroxyl radicals. While further studies have to determine which

explanation holds, vicious cycles appear plausible under such excessive conditions causing an exploding emergence of ROS. Most importantly, however, these data demonstrate that damage - specially to brain mitochondria - by cuprous Cu^{1+}, is an early event as reflected by MMP loss and structural alterations, whereas increased mitochondrial ROS appear to be a secondary consequence rather than a cause of organelle impairment.

On the contrary, we observed a Cu^{1+} dose-dependent decrease in free protein thiols in liver and brain mitochondria, already apparent at low Cu^{1+} challenges (Fig. 6). In agreement with suggestions that copper may specifically attack susceptible proteins at their thiol groups (Nakamura, 1972). Furthermore, this is in line with our earlier identification of mitochondrial membrane proteins that were sensitive to copper induced modifications of their cysteine residues (Zischka et al., 2011). This suggested mechanism of copper-mediated protein impairment resembles "classical" protein damage by direct attack of target amino acid residues (e.g., cysteine and methionine) (Davies, 2016). Conformational changes and/or protein activity losses may occur (Mirzaei and Regnier, 2006), which are especially critical for proteins of the mitochondrial oxidative phosphorylation.

Why are brain mitochondria so vulnerable to such a mode of attack? A first answer is, because their content of protective GSH was found to be significantly lower than in liver mitochondria (Fig. 5B). This result was further validated at cellular level in SHSY5Y cells versus U87MG cells. In agreement with earlier reports (Arciello et al., 2005), we identified SHSY5Y mitochondria to be highly susceptible to copper in structural as well as functional aspects (Figs. 6, 7). In line with our findings on isolated brain mitochondria, we observed an early loss of free protein thiols in SHSY5Y mitochondria resulting in a decreased ATP production capacity. Importantly, we traced their high sensitivity to a decreased defense mechanism against copper as shown by the absence of metallothionein and reduced levels of intracellular GSH compared to U87MG cells (Fig. 8). In fact, previous reports have similarly described the absence of metallothionein isotypes 1 and 2 in neurons (Aschner, 1996; Thirumoorthy et al., 2011; West et al., 2008). Metallothionein is responsible for copper handling and storage, thereby diminishing the redox activity of free copper within cells. Thus, the lack of MT1/2 as well as the reduced protection against oxidative protein damage by GSH could explain the high susceptibility of SHSY5Y mitochondria to copper. From these data, it is tempting to speculate that astrocytes in WD patients' brains should be capable of buffering high amounts of copper quite longstanding, but overload of their storage capacity may lead to copper release that impairs neuronal function. This would provide a plausible explanation as to why neuronal symptoms are rather late occurring features in WD. While future studies have to validate this, it is interesting to note that despite a massively higher copper uptake in U87MG cells (Fig. 8B), it was the SHSY5Y cells that presented with mitochondrial damage (Figs. 6B, 7).

In conclusion, we identified SHSY5Y mitochondria to be highly susceptible to copper toxicity. We linked this high sensitivity to a decreased copper defense system in SHSY5Y cells and propose a copper-dependent attack on mitochondrial free protein thiols as the major mechanism of mitochondrial copper toxicity. In contrast, increased production of reactive oxygen species was only a late-stage event, occurring in severely damaged mitochondria.

Acknowledgments

Conflict of interest statement

The authors have declared that no conflict of interest exists.

Appendix A. Supplementary data

References

Ala, A., Walker, A.P., Ashkan, K., Dooley, J.S., Schilsky, M.L., 2007. Wilson's disease. Lancet 369, 397–408.

Arciello, M., Rotilio, G., Rossi, L., 2005. Copper-dependent toxicity in SH-SY5Y neuroblastoma cells involves mitochondrial damage. Biochem. Biophys. Res. Commun. 327, 454–459.

Aschner, M., 1996. The functional significance of brain metallothioneins. FASEB J. 10, 1129–1136.

Banci, L., Bertini, I., Ciofi-Baffoni, S., Kozyreva, T., Zovo, K., Palumaa, P., 2010. Affinity gradients drive copper to cellular destinations. Nature 465, 645–648.

Banci, L., Bertini, I., Ciofi-Baffoni, S., D'Alessandro, A., Jaiswal, D., Marzano, V., et al., 2011. Copper exposure effects on yeast mitochondrial proteome. J. Proteome 74, 2522–2535.

Bearn, A., Yü, T., Gutman, A., 1957. Renal function in Wilson's disease. J. Clin. Investig. 36, 1107.

Berman, S.B., Watkins, S.C., Hastings, T.G., 2000. Quantitative biochemical and ultrastructural comparison of mitochondrial permeability transition in isolated brain and liver mitochondria: evidence for reduced sensitivity of brain mitochondria. Exp. Neurol. 164, 415–425.

Bernardi, P., Vassanelli, S., Veronese, P., Colonna, R., Szabo, I., Zoratti, M., 1992. Modulation of the mitochondrial permeability transition pore. Effect of protons and divalent cations. J. Biol. Chem. 267, 2934–2939.

Bradford, M.M., 1976. A rapid and sensitive method for the quantitation of microgram quantities of protein utilizing the principle of protein-dye binding. Anal. Biochem. 72, 248–254.

Brose, J., La Fontaine, S., Wedd, A.G., Xiao, Z., 2014. Redox sulfur chemistry of the copper chaperone Atox1 is regulated by the enzyme glutaredoxin 1, the reduction potential of the glutathione couple GSSG/2GSH and the availability of Cu (I). Metallomics 6, 793–808.

Bull, P.C., Thomas, G.R., Rommens, J.M., Forbes, J.R., Cox, D.W., 1993. The Wilson disease gene is a putative copper transporting P-type ATPase similar to the Menkes gene. Nat. Genet. 5, 327–337.

Catana, A.M., Medici, V., 2012. Liver transplantation for Wilson disease. World J. Hepatol. 4, 5.

Ciriolo, M.R., Desideri, A., Paci, M., Rotilio, G., 1990. Reconstitution of Cu, Zn-superoxide dismutase by the Cu (I). glutathione complex. J. Biol. Chem. 265, 11030–11034.

Cumings, J., 1948. The copper and iron content of brain and liver in the normal and in hepato-lenticular degeneration. Brain 71, 410–415.

Członkowska, A., Schilsky, M., 2017. Wilson disease: brain pathology. Wilson Dis. 142, 77.

Das, A., Banik, N.L., Ray, S.K., 2008. Retinoids induced astrocytic differentiation with down regulation of telomerase activity and enhanced sensitivity to taxol for apoptosis in human glioblastoma T98G and U87MG cells. J. Neuro-Oncol. 87, 9–22.

Davies, M.J., 2016. Protein oxidation and peroxidation. Biochem. J. 473, 805–825.

Einer, C., Hohenester, S., Wimmer, R., Wottke, L., Artmann, R., Schulz, S., et al., 2017. Mitochondrial adaptation in steatotic mice. Mitochondrion 40, 1–12.

Ellman, G., Lysko, H., 1979. A precise method for the determination of whole blood and plasma sulfhydryl groups. Anal. Biochem. 93, 98–102.

Encinas, M., Iglesias, M., Liu, Y., Wang, H., Muhaisen, A., Cena, V., et al., 2000. Sequential treatment of SH-SY5Y cells with retinoic acid and brain-derived neurotrophic factor gives rise to fully differentiated, neurotrophic factor-dependent, human neuron-like cells. J. Neurochem. 75, 991–1003.

Fernández-Vizarra, E., Enríquez, J.A., Pérez-Martos, A., Montoya, J., Fernández-Silva, P., 2011. Tissue-specific differences in mitochondrial activity and biogenesis. Mitochondrion 11, 207–213.

Hackenbrock, C.R., 1966. Ultrastructural bases for metabolically linked mechanical activity in mitochondria I. Reversible ultrastructural changes with change in metabolic steady state in isolated liver mitochondria. J. Cell Biol. 30, 269–297.

Hosseini, M.-J., Shaki, F., Ghazi-Khansari, M., Pourahmad, J., 2014. Toxicity of copper on isolated liver mitochondria: impairment at complexes I, II, and IV leads to increased ROS production. Cell Biochem. Biophys. 70, 367–381.

Hunter, D.R., Haworth, R.A., 1979. The Ca2 + −induced membrane transition in mitochondria I. The protective mechanisms. Arch. Biochem. Biophys. 195, 453–459.

Kessler, R.J., Tyson, C.A., Green, D.E., 1976. Mechanism of uncoupling in mitochondria: uncouplers as ionophores for cycling cations and protons. Proc. Natl. Acad. Sci. 73, 3141–3145.

Kim, B.-E., Nevitt, T., Thiele, D.J., 2008. Mechanisms for copper acquisition, distribution and regulation. Nat. Chem. Biol. 4, 176–185.

Knöpfel, M., Solioz, M., 2002. Characterization of a cytochrome b(558) ferric/cupric reductase from rabbit duodenal brush border membranes. Biochem. Biophys. Res. Commun. 291, 220–225.

Korshunov, S.S., Skulachev, V.P., Starkov, A.A., 1997. High protonic potential actuates a mechanism of production of reactive oxygen species in mitochondria. FEBS Lett. 416, 15–18.

Lai, J.C., Blass, J.P., 1984. Neurotoxic effects of copper: inhibition of glycolysis and glycolytic enzymes. Neurochem. Res. 9, 1699–1710.

Lichtmannegger, J., Leitzinger, C., Wimmer, R., Schmitt, S., Schulz, S., Kabiri, Y., et al., 2016. Methanobactin reverses acute liver failure in a rat model of Wilson disease. J.

Clin. Invest. 126, 2721–2735.

Litwin, T., Gromadzka, G., Szpak, G., Jabłonka-Salach, K., Bulska, E., Członkowska, A., 2013. Brain metal accumulation in Wilson's disease. J. Neurol. Sci. 329, 55–58.

Lorincz, M.T., 2010. Neurologic Wilson's disease. Ann. N. Y. Acad. Sci. 1184, 173–187.

Mirzaei, H., Regnier, F., 2006. Creation of allotypic active sites during oxidative stress. J. Proteome Res. 5, 2159–2168.

Mootha, V.K., Bunkenborg, J., Olsen, J.V., Hjerrild, M., Wisniewski, J.R., Stahl, E., et al., 2003. Integrated analysis of protein composition, tissue diversity, and gene regulation in mouse mitochondria. Cell 115, 629–640.

Murphy, M.P., 2009. How mitochondria produce reactive oxygen species. Biochem. J. 417, 1–13.

Nakamura, M., 1972. Yamazaki I. One-electron transfer reactions in biochemical systems. VI. Changes in electron transfer mechanism of lipoamide dehydrogenase by modification of sulfhydryl groups. Biochimica et Biophysica Acta (BBA)-Bioenergetics 267, 249–257.

Nicholls, D.G., Ferguson, S.J., 1992. Bioenergetics 2. Academic Press.

Pfeiffer, R.F., 2007. Wilson's disease. Semin. Neurol. 27, 123–132.

Rae, T., Schmidt, P., Pufahl, R., Culotta, V., O'halloran, T., 1999. Undetectable intracellular free copper: the requirement of a copper chaperone for superoxide dismutase. Science 284, 805–808.

Rahman, I., Kode, A., Biswas, S.K., 2006. Assay for quantitative determination of glutathione and glutathione disulfide levels using enzymatic recycling method. Nat. Protoc. 1, 3159–3165.

Roberts, E.A., Schilsky, M.L., 2008. Diagnosis and treatment of Wilson disease: an update. Hepatology 47, 2089–2111.

Roberts, E.A., Robinson, B.H., Yang, S., 2008. Mitochondrial structure and function in the untreated Jackson toxic milk (tx-j) mouse, a model for Wilson disease. Mol. Genet. Metab. 93, 54–65.

Schmitt, S., Saathoff, F., Meissner, L., Schropp, E.-M., Lichtmannegger, J., Schulz, S., et al., 2013. A semi-automated method for isolating functionally intact mitochondria from cultured cells and tissue biopsies. Anal. Biochem. 443, 66–74.

Schulz, T.J., Thierbach, R., Voigt, A., Drewes, G., Mietzner, B., Steinberg, P., et al., 2006. Induction of oxidative metabolism by mitochondrial frataxin inhibits cancer growth Otto Warburg Revisited. J. Biol. Chem. 281, 977–981.

Schulz, S., Schmitt, S., Wimmer, R., Aichler, M., Eisenhofer, S., Lichtmannegger, J., et al., 2013. Progressive stages of mitochondrial destruction caused by cell toxic bile salts. Biochim. Biophys. Acta 1828, 2121–2133.

Schulz, S., Lichtmannegger, J., Schmitt, S., Leitzinger, C., Eberhagen, C., Einer, C., et al., 2015. A protocol for the parallel isolation of intact mitochondria from rat liver, kidney, heart, and brain. In: Proteomic Profiling: Methods and Protocols, pp. 75–86.

Schumacher, G., Platz, K., Mueller, A., Neuhaus, R., Luck, W., Langrehr, J., et al., 2001. Liver transplantation in neurologic Wilson's disease. Transplant. Proc. 33, 1518–1519.

Shipley, M.M., Mangold, C.A., Szpara, M.L., 2016. Differentiation of the SH-SY5Y human neuroblastoma cell line. J. Visualized Exp. 53193.

Speisky, H., Gómez, M., Burgos-Bravo, F., López-Alarcón, C., Jullian, C., Olea-Azar, C., et al., 2009. Generation of superoxide radicals by copper-glutathione complexes: redox-consequences associated with their interaction with reduced glutathione. Bioorg. Med. Chem. 17, 1803–1810.

Sternlieb, I., 1968. Mitochondrial and fatty changes in hepatocytes of patients with Wilson's disease. Gastroenterology 55, 354–367.

Sternlieb, I., 1978. Electron microscopy of mitochondria and peroxisomes of human hepatocytes. Prog. Liver Dis. 6, 81–104.

Sternlieb, I., Feldmann, G., 1976. Effects of anticopper therapy on hepatocellular mitochondria in patients with Wilson's disease. Gastroenterology 71, 457–461.

Stohs, S.J., Bagchi, D., 1995. Oxidative mechanisms in the toxicity of metal ions. Free Radic. Biol. Med. 18, 321–336.

Tanzi, R., Petrukhin, K., Chernov, I., Pellequer, J., Wasco, W., Ross, B., et al., 1993. The Wilson disease gene is a copper transporting ATPase with homology to the Menkes disease gene. Nat. Genet. 5, 344–350.

Thirumoorthy, N., Sunder, A.S., Kumar, K.M., Ganesh, G., Chatterjee, M., et al., 2011. A review of metallothionein isoforms and their role in pathophysiology. World J. Surgical Oncol. 9, 54.

Valko, M., Rhodes, C.J., Moncol, J., Izakovic, M., Mazur, M., 2006. Free radicals, metals and antioxidants in oxidative stress-induced cancer. Chem. Biol. Interact. 160, 1–40.

Vogel, F.S., Evans, J.W., 1961. Morphologic alterations produced by copper in neural tissues with consideration of the role of the metal in the pathogenesis of Wilson's disease. J. Exp. Med. 113, 997–1004.

Vogel, F.S., Kemper, L., 1963. Biochemical reactions of copper within neural mitochondria, with consideration of the role of the metal in the pathogenesis of Wilson's disease. Lab. Inves. 12, 171–179.

Walshe, J.M., 2007. Cause of death in Wilson disease. Mov. Disord. 22, 2216–2220.

Wang, Y., Sun, H., Ru, Y., Yin, S., Yin, L., Liu, S., 2011. Proteomic survey towards the tissue-specific proteins of mouse mitochondria. Sci. China Life Sci. 54, 3–15.

Weiss, K.H., Schäfer, M., Gotthardt, D.N., Angerer, A., Mogler, C., Schirmacher, P., et al., 2013. Outcome and development of symptoms after orthotopic liver transplantation for Wilson disease. Clin. Transpl. 27, 914–922.

West, A.K., Hidalgo, J., Eddins, D., Levin, E.D., Aschner, M., 2008. Metallothionein in the central nervous system: Roles in protection, regeneration and cognition. Neurotoxicology 29, 489–503.

Xing, F., Luan, Y., Cai, J., Wu, S., Mai, J., Gu, J., et al., 2017. The anti-warburg effect elicited by the cAMP-PGC1α pathway drives differentiation of glioblastoma cells into astrocytes. Cell Rep. 18, 468–481.

Zamzami, N., Métivier, D., Kroemer, G., 2000. Quantitation of mitochondrial transmembrane potential in cells and in isolated mitochondria. Methods Enzymol. 322, 208.

Zhou, M., Diwu, Z., Panchuk-Voloshina, N., Haugland, R.P., 1997. A stable nonfluorescent derivative of resorufin for the fluorometric determination of trace hydrogen peroxide: applications in detecting the activity of phagocyte NADPH oxidase and other oxidases. Anal. Biochem. 253, 162–168.

Zischka, H., Lichtmannegger, J., 2014. Pathological mitochondrial copper overload in livers of Wilson's disease patients and related animal models. Ann. N. Y. Acad. Sci. 1315, 6–15.

Zischka, H., Larochette, N., Hoffmann, F., Hamöller, D., Jägemann, N., Lichtmannegger, J., et al., 2008. Electrophoretic analysis of the mitochondrial outer membrane rupture induced by permeability transition. Anal. Chem. 80, 5051–5058.

Zischka, H., Lichtmannegger, J., Schmitt, S., Jägemann, N., Schulz, S., Wartini, D., et al., 2011. Liver mitochondrial membrane crosslinking and destruction in a rat model of Wilson disease. J. Clin. Invest. 121, 1508–1518.